

Recent developments in support materials for use in high performance liquid chromatography.

by David McCalley, Centre for Research in Biosciences, University of the West of England, Bristol BS16 1 QY U.K.

A number of advances have taken place in the last decade in the area of support materials for high performance liquid chromatography (HPLC). These developments have included the use of very small porous particles (< 2.0 μm diameter), new types of superficially porous or "shell" particles and the development of a second generation of silica monolithic columns with increased efficiency compared with earlier versions. New formats such as pillar arrays offer interesting possibilities as future support materials. This paper will consider these developments mostly with regard to their use in the analysis of small molecules.

Very small particle/shell particle columns.

The potential of small particles for use in HPLC has been recognised for a long time. However, only in the last 10 years or so since the introduction of commercial instruments capable of high pressure operation together with low extra-column band spreading properties, has it become possible to exploit the advantages of these particles. Small particles give rise to higher efficiency for the same column length, but their benefit is principally in generating similar efficiencies to larger particle columns in a shorter analysis time. A 25 cm column of 5.0 μm totally porous particles may generate 25,000 theoretical plates, which should also be readily achieved on an 8.5 cm column of similar 1.7 μm particles, assuming a reduced plate height $h = 2$ in both cases. As the 1.7 μm column is only about one third of the length, it should produce results 3x faster than the large particle column. The optimum flow rates of small particle columns are also higher, so considerably greater increases in speed are possible. Shorter retention means less solvent consumption. As high pressure instruments are designed with low extra-column bandspreading, narrower columns can also be used e.g. a 2.1 mm i.d. column operated at the same flow velocity uses approximately one fifth the solvent of a 4.6 mm column. Thus further reductions in solvent consumption result. The smallest commercial particles have a particle diameter of 1.3 μm but optimum flow may not be reached due to pressure limitations even if relatively short (e.g. 5 cm) columns are used. The advantages of small particle columns can be further enhanced by the use of small shell particles instead of totally porous materials, which have a coating of porous material surrounding a solid non-porous core [1].

The use of very small particle columns is, however, not without practical difficulties. The most obvious consequence is the higher back pressure generated. As pressure is inversely proportional to the particle diameter squared, a 1.7 μm column requires ~ 9 times the pressure compared with a 5.0 μm particle column operated at same flow

velocity, necessitating pumps of improved capability. Other difficulties, such as frictional heating and selectivity differences may also result (see below).

Core shell particles. Preparation. These particles are now available from most HPLC column manufacturers. Although methods of preparation differ in their details, two common approaches are outlined in Fig. 1 [2]. The layer by layer process consists of adding a cationic polymer to solid silica cores (made by the Stoeber process) held at high pH such that the silanols are negatively charged. After elimination of excess material, a suspension of silica nanoparticles of size 10-16 nm is added and the process is repeated many times until the desired shell thickness is achieved. An alternative procedure is to apply a polymer to the cores that can absorb several layers of sol particles, such that the porous shell grows from 5-10 layers at a time. This process has been modified into a 1-step coacervation procedure shown in Fig. 1. In each approach, the polymer is finally removed by burning, and the particles are sintered to improve their mechanical properties. Another method involving a one pot synthesis, is the sphere on sphere process [3] where silica microspheres are coated with a single layer of nanospheres (Fig. 2). The surface of this material has very small pores with diameter < 2 nm but its significant porosity, allowing use for the separation of large proteins, results from the spaces between the surface nanospheres.

Efficiency. It is often proposed that a $2.7 \mu\text{m}$ shell column has “the same performance as a sub- $2 \mu\text{m}$ porous column but at around half the back pressure”. This statement is rather confusing because column porosity does not affect its back pressure: the pores are too small to allow flow through them, which takes place instead principally around the particles. Thus shell and porous columns of same particle diameter (d_p) generate similar back pressure. The lower back pressure of a $2.7 \mu\text{m}$ shell particle is merely due to its larger d_p . The effect arises instead due to the smaller minimum reduced plate height (h) of shell particles (as low as 1.2-1.5) compared with totally porous particles (typically 1.9-2.1). This improved efficiency could be due to :

(i) The smaller particle size distribution of shell particles (rsd 5% compared with 20% for totally porous particles).

(ii) More likely it is due principally to the superior packing of shell particles (reduction in the A term of the van Deemter equation); to a lesser extent, reduction in the B term contributes due to there being less mobile phase in column; there may also be some reduction in the C term especially for large molecules due to the reduced diffusion distance, although this effect is considered small for small molecules with higher diffusivity.

(iii) Shell columns have less problems with frictional heating due to the greater thermal conductivity of the solid core compared with the mobile phase it replaces in porous silica. This property allows the use in some circumstances of larger 4.6 mm i.d columns of $\sim 2.5 \mu\text{m}$ shell particles in place of 2.1 mm columns of sub- 2 micron particles. The use of larger diameter shell columns may even be advantageous, as wider bore columns are generally easier to pack, and they are also more tolerant of instrument band spreading (see below).

Sub 2 μ m shell particle columns are increasingly used to obtain higher efficiencies than totally porous particle columns at similar pressures.

Possibility of overloading effects. Fig. 3 shows the structure of a typical shell particle (Halo, Advanced Materials Technology) with $d_p = 2.7 \mu\text{m}$ and shell thickness 0.5 μm . While the typical two dimensional representation of the structure of these particles is misleading, a true spherical three-dimensional consideration reveals that they can be considered to have a rather thick shell. Indeed the non-porous fractional volume of the particle can be calculated using simple geometry as occupying only 25% of the total, implying that the porous volume is 75% of that of a totally porous particle of the same diameter. These dimensions are in stark contrast to those of the early “pellicular” particles which contained only a very small fraction of porous material. Thus, there is no particular reason to suspect that modern shell particles should be prone to overloading. Of course, particles with thinner porous shells have been developed especially for the analysis of large molecules such as proteins, where slow diffusion in and out of a thick shell may compromise column efficiency. These particles may have somewhat reduced loadability. Another factor to consider is that the surface area of the porous material in a shell column may not be the same as that in a totally porous column, due (at least) to their different methods of manufacture. Fig. 4 shows a practical comparison of the loading capacity of a totally porous Zorbax C18 and a Poroshell column both from the same manufacturer (Agilent). The basic probe nortriptyline has been shown to overload readily on C18 columns at low pH (e.g. ammonium formate buffer pH 3.0 as used here) [4]. The overloading effect is shown by reduction in efficiency as the concentration of injected solute increases. As this reduction in efficiency varies with the retention factor k of the solute, particularly at low values of k , a constant high value ($k = 10$) was used in these experiments by adjusting the concentration of organic modifier (acetonitrile) in the mobile phase. For both columns, overloading is reduced as the concentration of buffer in the mobile phase increases. The summary Table below Fig. 4 shows the concentration of solute necessary to reduce the small sample concentration efficiency (N_0) by one half ($C_{0.5}$) for the totally porous column ($d_p = 1.8 \mu\text{m}$) and three types of shell column ($d_p \sim 2.5 \mu\text{m}$). All columns gave good peak shape (asymmetry factor $A_s \sim 1$) for small sample mass. $C_{0.5}$ is shown to be approximately the same for all these columns, indicating that there are no major differences in loading capacity. Similar results were obtained also for other solutes [4].

Effects of Instrumental Bandspreading

The effects of instrumental bandspreading are much greater for small volume peaks generated by short, narrow, high efficiency columns. This can be seen from a consideration of equation 1.

$$\sigma_{\text{experimental}}^2 = \sigma_{\text{column}}^2 + \sigma_{\text{extracolumn}}^2 \quad (1)$$

where $\sigma_{\text{experimental}}^2$ is the measured peak variance, σ_{column}^2 is the variance caused by the column alone, and $\sigma_{\text{extracolumn}}^2$ is the extracolumn variance (all values usually measured in μl^2). The inherent column variance (and from this its efficiency) can be calculated from the measured experimental variance by measuring the extracolumn bandspreading by substitution of a zero dead volume (ZDV) connector in place of the column. However, this

procedure has become the subject of some controversy. For example, extracolumn effects are measured at low (atmospheric) pressure, whereas the experimental value is measured at high pressure (with the column in place). Under the latter condition, the viscosity of the mobile phase may be increased somewhat leading to reduced solute diffusion in the mobile phase, and an underestimation of the extracolumn contribution. A further problem is that the peak variance is usually measured by considering the peak width at a single position at some proportion of the peak height (such as the 5 sigma width at 4.4% of peak height). Desmet has proposed an improved deconvolution method for subtracting the shape of the extra column peak in its entirety from the experimentally measured peak shape [5]. It remains to be seen however, if this procedure will be universally adopted. Fig. 5 shows measurements of the extra column bandspreading of an Acquity classic high pressure mixing binary UHPLC system, using the classical ZDV method and the 5-sigma peak width. The upper plot, (using a sufficiently high data gathering rate of 80Hz), shows that the extracolumn variance increases with increase of flow rate until a broad maximum value is achieved. At low flow rate, radial inhomogeneity of the flow profile can be counteracted by solute diffusion between the various flow streams. Using 90 % ACN in the mobile phase, the bandspreading amounts to $\sim 3.5 \mu\text{L}^2$ at a flow rate of 0.5 mL/min, a flow typically used with very small particle columns of i.d. 2.1 mm. A somewhat greater bandspreading value is obtained by use of 10 % ACN as the mobile phase, a solvent of greater viscosity which reduces solute diffusion in the mobile phase. The lower plot of Fig. 5 shows additionally the importance of using a suitably fast data gathering rate / small time constant in these experiments. A value of 20 HZ is clearly insufficient for such experiments. A similar experiment indicated instrumental bandspreading of $25 \mu\text{L}^2$ for a conventional HPLC system (Agilent 1100) adapted with the use of small diameter connecting tubing (0.12 mm i.d) and a micro flow cell (1 μL). Using these values for 10 cm columns with i.d. 2.1 mm and 4.6 mm, of true efficiency 25000 plates operated on the two systems, the % loss in column efficiency (N) caused by the instrumental bandspreading can be estimated (Fig. 6). A 0.21 cm i.d. column operated on the Acquity system would show a loss of 40 % in efficiency for a peak of $k = 1$, about double the value for the 0.46 cm column operated on the (much older) Agilent system! This result indicates clearly the problems of operation of high efficiency, narrow bore columns even on modern UHPLC systems with apparently small extracolumn band broadening contribution. Operation of the 0.46 cm column on the Acquity system shows understandably few problems; even with an unretained peak, the loss in N is $\sim 10\%$. Furthermore, losses in efficiency decrease as the retention of the solute increases, as the inherent band broadening caused by the column becomes large compared with the instrumental effects. Nevertheless, problems are increased if a shorter 5cm column with the same reduced plate height is used (lower plot Fig. 6) as the variance due to the column is reduced. Note that it is possible to use the wider 0.46 cm columns packed with shell particles of $\sim 2.5 \mu\text{m}$ diameter as there are less problems with frictional heating with this type of phase (see below).

Frictional heating effects.

Frictional heating is caused by percolation of the mobile phase through the packed bed. The power P generated in watts within the column is given by

$$\text{Power} = \Delta P \times F \quad (2)$$

where ΔP is the pressure drop (in SI units N/m^2) and F is the volumetric flow rate (m^3/s) through the column. The heating effect produced can give rise to both axial and radial temperature gradients in the column. Axial temperature gradients are formed with temperature generally increasing further down the column length. These can lead to changes in solute retention; in reversed-phase separations, a decrease in retention is usually observed. Radial temperature gradients are caused by loss of heat through the column walls causing the centre of the column to be at higher temperature than the wall region. Thus, a spread of velocities across the column radius occurs, that can lead to serious band broadening. Usually, the column is maintained in as adiabatic an environment as possible, to restrict heat losses and minimise the radial temperature gradient, although such an approach tends to maximise the axial gradient. The use of narrower bore columns (e.g. 2.1 mm i.d. rather than 4.6 mm) is commonly used as the power generated is less, and the surface area to volume ratio of the column is greater, promoting heat dissipation. Shell particles also promote heat dissipation due to the higher thermal conductivity of the solid core compared with porous materials containing typical HPLC solvents.

Effect of pressure and temperature on selectivity

Pressure considered in isolation from other effects can cause important selectivity changes. For example, pressure increases from 100-1100 bar can cause increases in retention that range from 8-30 times for insulin (MW ~6 kDa) to myoglobin (30 kDa) in isocratic RP separations [6]. The effect of pressure in the absence of frictional heating can be measured by attaching restriction capillaries of small i.d. to the end of the column while maintaining the flow rate constant. The increase in retention with pressure may be caused by the compressibility of solutes which result in them occupying less volume in the stationary phase than in the mobile phase. Large molecules may be more compressible than small molecules, explaining the greater increases in retention that have been noted. Nevertheless, increases in k of 50% for 500 bar pressure increase can occur also for smaller molecules (MW < 500, [7]). Fig. 7 shows some pronounced changes in selectivity for a mixture of small neutral molecules (e.g. nitrobenzene and acetophenone) together with some larger polar or ionised compounds (e.g. prednisone and diphenhydramine) on a short (5 cm) ODS column containing 5 μm particles at low pressure (no restriction capillary) and at pressures up to 811 bar achieved by adding restriction capillaries to the end of the column. The use of a short, relatively large particle column ensures that the pressure drop across the column itself is small, regardless of the total pressure, and thus that frictional heating effects are negligible. While for example nitrobenzene shows relatively little increase in retention with pressure, diphenhydramine shows considerable increases. Thus it elutes just after nitrobenzene at low pressure, but co-elutes with nitrobenzene at the highest pressure used. Other studies have increased the pressure

merely by increasing the flow rate, which results in a concurrent increase in the column temperature by frictional heating, especially when very small particle columns are used. As increased temperature generally results in reduced retention in reversed-phase chromatography, the effects act in opposite directions, giving some moderation in changes in retention. However, in hydrophilic interaction chromatography, increased pressure can reduce retention, giving pronounced loss of retention when flow rate is increased, as both effects operate in the same direction [8].

Monolithic Columns.

This section will concentrate on monolithic columns based on silica. Organic monoliths have found much success for the analysis of large biological molecules, but have not seen much application in the separation of small molecules. Monolithic silica columns were developed in the 1990s and commercialized in 2000. They had the potential to outperform the packed columns of the time. The first commercialized monolithic silica column clad with PEEK, Chromolith Performance RP-18e (4.6 mm ID, 10 cm), had the efficiency as a column packed with 3.5-4 μm particles but with a pressure drop (or permeability) equivalent to a column packed with 7-8 μm particles. They are prepared by hydrolytic polymerisation of e.g. tetramethoxysilane in aqueous acetic acid in the presence of polyethylene glycol (PEG). Mesopores in the structure are formed by treatment with aqueous ammonia. First generation monolithic silica columns (rod and capillary) had ca. 2-8 μm through-pores and 1-2 μm skeletons, which were too large to generate high efficiency and the external porosity was too high. Through pores even of 2 μm resulted in a large mobile-phase mass transfer contribution to band broadening. A dilemma however exists if improvement in efficiency is desired-reduction in the size of the through pores and skeleton will decrease the permeability, this being one of the original advantages of the monolith structure. In so-called "second generation monoliths" the size of the through pores (1.1-1.2 μm) was decreased by ~40% in Chromolith HR compared with the first generation "Chromolith Performance". The additional improved radial homogeneity in the structure from the centre to the outer portion has resulted in a claimed increase in column efficiency of up to 50 % compared with the first generation columns, with H values as low as 5 μm . This value would suggest that up to 20,000 theoretical plates could be expected in a 10 cm column. However, about 2.5 times the pressure is required to achieve the same flow velocity compared with first generation monoliths. An advantage of monolith columns is the absence of retaining frits that are necessary in particle packed columns. This lack of frits could partially explain the claimed resistance of monoliths to samples with a high concentration of matrix compounds. The structure of a hybrid capillary silica monolith is shown in Fig. 8; note the apparently excellent radial and structural homogeneity of the phase [9].

Monoliths have suffered from competition with very small particle packed and especially shell columns; their performance particularly for fast analysis is inferior. A problem with the rod form of monoliths of i.d. comparable to typical packed HPLC columns (i.d. 2-5 mm) is the necessity of enclosing or cladding the structure in a suitable material such as polyether ether ketone (PEEK) without leaving void spaces that could disrupt the radial flow profile of the column and thus cause deterioration in efficiency. The stability of typical cladding

procedures to high pressure is considerably less than that of stainless steel particulate columns, being typically only 200-300 bar. Further efforts are necessary to improve the efficiency of monoliths without increasing the back pressure, for instance by further enhancements in the homogeneity of the structure of the material. Nevertheless, there may be a demand for the use of long capillary monoliths for the separation of complex biological samples e.g. in peptide analysis, where columns of length several meters can generate over 1 million theoretical plates at acceptable back pressures.

Polymer monolith columns complement silica-based monoliths in that they have been applied to the separation of high molecular weight solutes and biologically active compounds. The interested reader is directed to an excellent review of these materials recently published by Svec and Lv [10].

Pillar array columns.

Pillar array columns were first proposed in 1998 for use under electrically driven flow. A pillar array is a 2-dimensional equivalent of the sphere packing in a packed bed. It is produced by micro-machining in silicon or glass, and has the advantage that the pillars can be arranged in a perfectly ordered and reproducible array, offering a dramatic reduction in eddy dispersion. Long columns (3m) with optimal pillar diameters (5 μm) and interpillar distance (2.5 μm) could produce 1 million plates with a pressure restricted to 350 bar. Desmet and co-workers showed a radially elongated pillar array (REP) can produce the same separation performance as open-tubular columns, which are often regarded as the optimum possible column format [11]. A monolayer of octylsilane can be coated on the external surface of the pillars. In REP columns the pillars have a radially elongated (see Fig. 9), diamond shape as opposed to cylindrical shape, which is the 2D equivalent of spheres. The REP variant of pillar columns leads to a significant reduction in the minimum plate height. With length 4cm, it was possible to achieve 160,000 theoretical plates for unretained analytes and 70,000 plates for retained analytes, despite the relatively large interpillar distance (2.5 μm). While pillar array columns offer promise for the future, there are still difficulties to overcome in terms of the small sample capacity of the material, and problems with deactivating the surface such that it is suitable for the analysis of more "active" compounds.

Conclusions.

Small particle columns operated at high(er) pressures can generate the same efficiency as conventional HPLC columns with considerably reduced analysis time and solvent consumption.

Shell particles give further performance enhancements allowing use of somewhat larger $\sim 2.5 \mu\text{m}$ particles at lower pressures instead of sub- $2 \mu\text{m}$ particles, or to give increased efficiency for sub- $2 \mu\text{m}$ particles .

Shell particles seem to have few disadvantages even with regard to overloading and are currently the best choice for fast efficient separations.

Second generation silica monoliths give improved efficiency over first generation materials due to smaller through pores/skeletons. However, this improved efficiency is at the expense of higher back pressure.

Pillar array columns offer exciting future possibilities.

Acknowledgements

The author thanks Dr Bill Barber (Agilent Technologies) for provision of Fig.1; the authors of ref. [3] for Fig. 2 and the authors of ref. [9] for Fig. 9.

References

- [1] N. Tanaka, D.V. McCalley, *Anal. Chem.* 88 (2016) 279-298.
- [2] W. Chen, K. Jiang, A. Mack, B. Sachok, X. Zhu, W.E. Barber, X. Wang, *J. Chromatogr. A* 1414 (2015) 147-157.
- [3] R. Hayes, P. Myers, T. Edge, H.F. Zhang, *Analyst* 139 (2014) 5674-5677.
- [4] M.M. Fallas, S.M. C. Buckenmaier, D.V. McCalley, *J. Chromatogr. A* 1235 (2012) 49-59.
- [5] K. Vanderlinden, K. Broekhoven, Y. Vanderheyden, G. Desmet, *J. Chromatogr. A* 1442 (2016) 73-82.
- [6] S. Fekete, J.L. Veuthey, D.V. McCalley, D. Guillarme *J. Chromatogr. A* 1270 (2012)127-138.
- [7] M.M. Fallas, N. Tanaka, S.M.C. Buckenmaier, D. V. McCalley, *J. Chromatogr. A* 1297 (2013) 37-45.
- [8] J.C. Heaton, X. Wang, W.E. Barber, S.M.C. Buckenmaier, D.V. McCalley, *J. Chromatogr. A* 1328 (2014) 7-15.
- [9] H. Lin, L. Chen, J. Ou, Z. Liu, H.W. Wang, J. Dong, H. Zou, *J. Chromatogr. A* 1416 (2015) 74-82.
- [10] F. Svec, Y. Lv, *Anal. Chem.* 87 (2015) 250-273.
- [11] G. Desmet, M. Callewaert, H. Ottevaere, W. De Malsche, *Anal. Chem.* 87 (2015) 7382-7388

Legend to Figures.

Fig. 1 (Upper) Layer by layer process and (lower) coacervation process for production of shell particles.

Fig. 2 Scanning electron micrograph of sphere-on sphere particles.

Fig. 3 Dimensions of a Halo superficially porous particle.

Fig. 4 Comparison of loading with nortriptyline on totally porous (Zorbax) and shell ODS columns (Poroshell) from same manufacturer. Mobile phase: acetonitrile-ammonium formate buffer pH 3. Table shows small mass peak asymmetry (A_s) and efficiency (N_o , plates) together with concentration necessary to reduce N_o to half its value ($N_{0.5}$). Sample volume 1 μL .

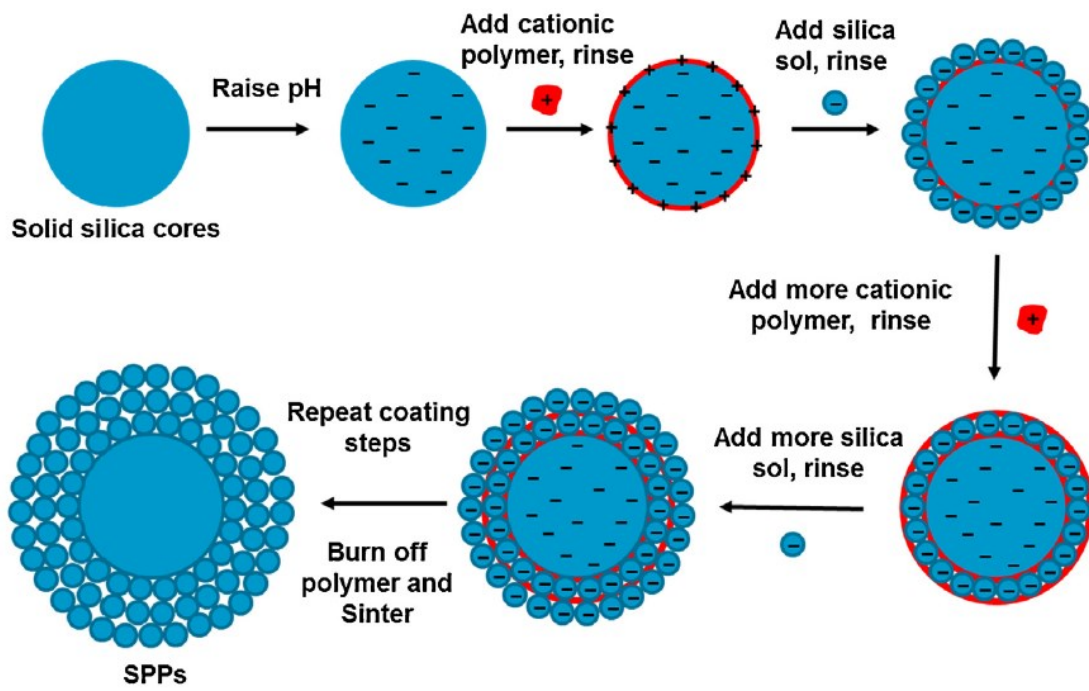
Fig. 5 (Upper) Measurement of instrumental band broadening of Acquity Classic UHPLC system using different probes/mobile phases. (Lower) Measurement of band broadening for naphthopyrene in 90 % acetonitrile at fast and low data gathering rates.

Fig. 6 Comparison of efficiency losses on columns of different length and i.d. on Acquity classic UHPLC system and Agilent 1100 for peaks of $k = 1$ to 10. The instrumental bandspreading of the Acquity system (AQ) was taken as $\sigma^2 = 3.5 \mu\text{L}^2$ and for the Agilent 1100 system (AG) as $\sigma^2 = 25 \mu\text{L}^2$.

Fig. 7 Changes with selectivity with pressure on a 5cm C18 column of 5 μm particles. Mobile phase: 25 % acetonitrile in phosphate buffer pH 2.7. Peak identities: 1 = uracil, 2 = aniline, 3 = naphthalene-2-sulfonic acid, 4 = propranolol, 5 = prednisone, 6 = acetophenone, 7 = diphenhydramine, 8 = nitrobenzene.

Fig. 8 Scanning electron micrograph of a hybrid organic silica monolith.

Fig. 9 Top view of pillar arrangement and velocity field of (a) a conventional cylindrical pillar array and (b) a radially elongated pillar column. The white arrow L_x indicates the net direction of flow; white arrow L_i indicates the direction of flow along the tortuous path followed by the liquid. Reprinted with permission from G. Desmet, M. Callewaert, H. Ottevaere, W. De Malsche, *Anal. Chem.* 87 (2015) 7382-7388. Copyright 2015, American Chemical Society.



Urea, formaldehyde polymerization coats sol and core
 Coated sol then adsorbs to coated core.

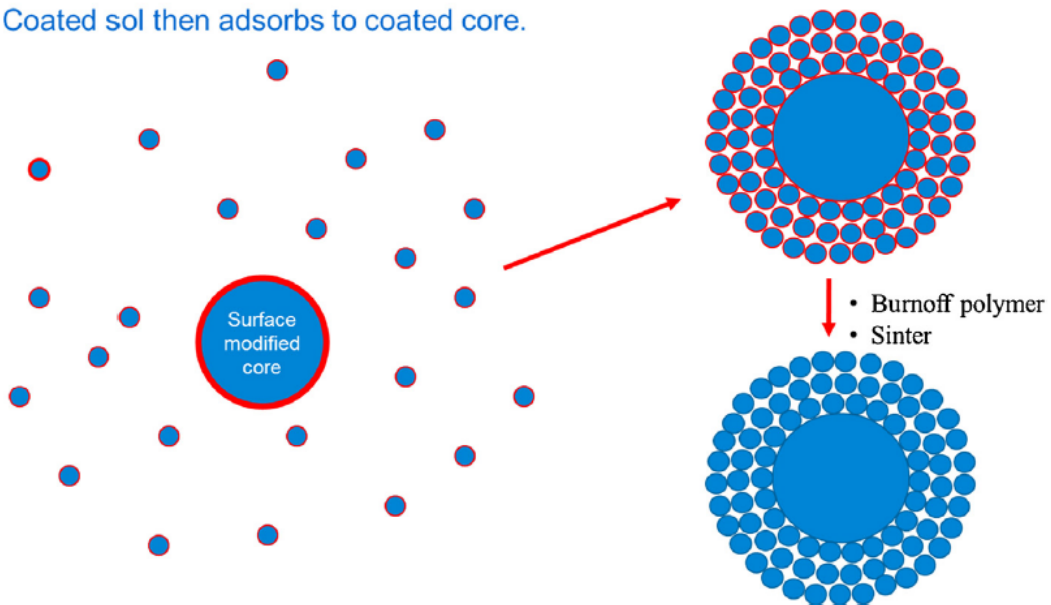


Fig 1

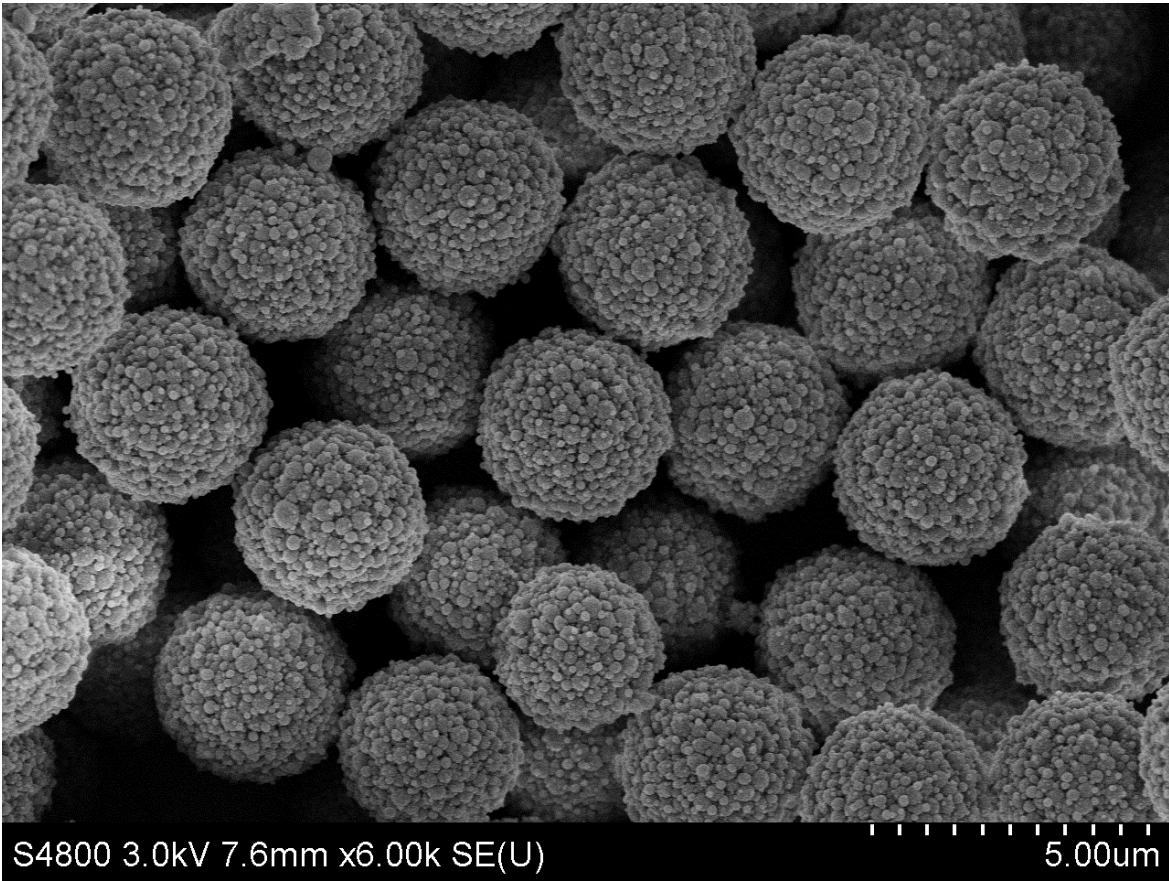


Fig 2

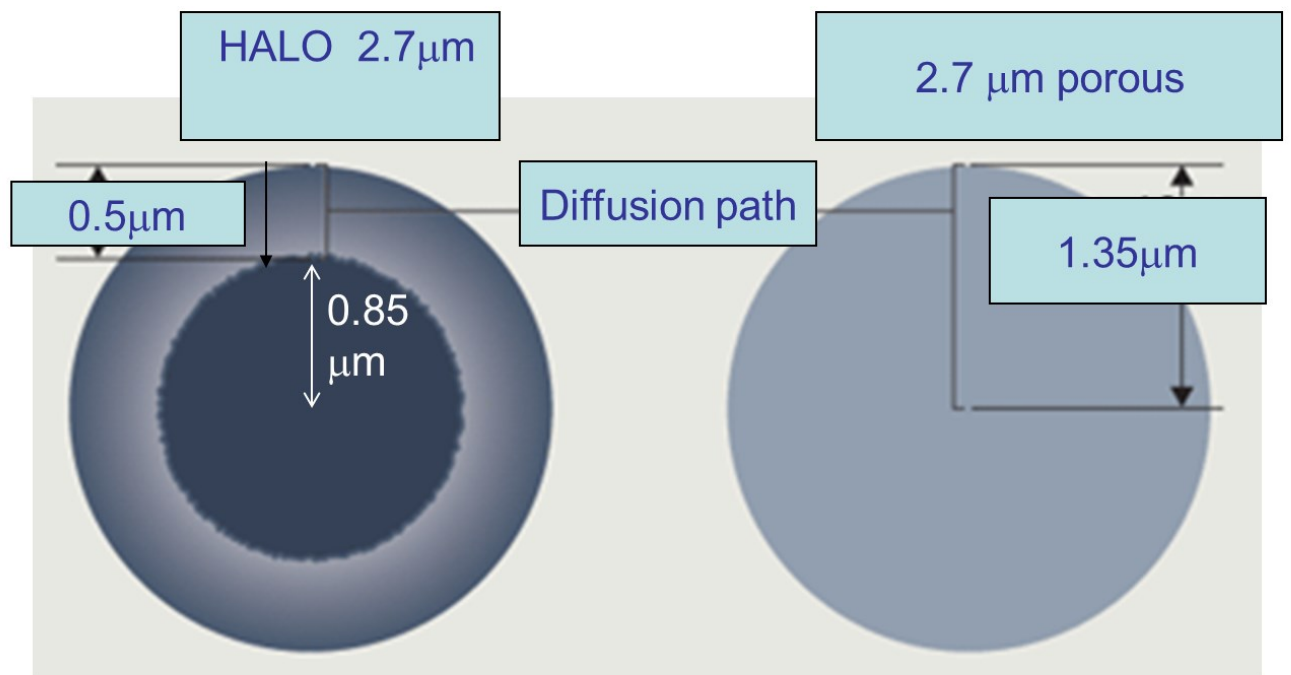
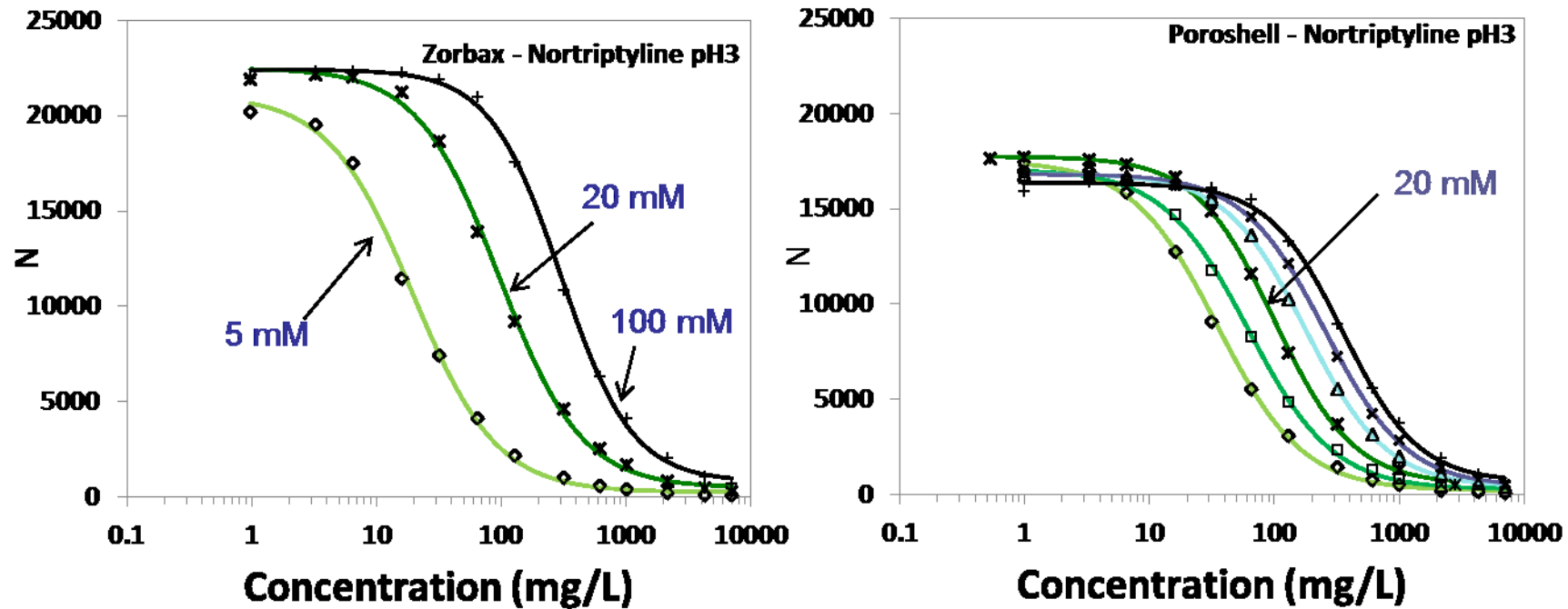


Fig. 3

Fig. 4

Comparison of Loading with Nortriptyline (BH⁺) on totally porous and shell columns from same manufacturer (1 μ L injections). Buffer (ammonium formate) concentrations 5-100 mM.



Column	Buffer (mM)	A_s (small conc)	N_0	$C_{0.5}$ (mg/L)	
Zorbax	10 x 0.21	20	1.07	22 500	97
Poroshell	10 x 0.21	20	1.08	17 700	100
Kinetex	10 x 0.21	20	0.90	17 700	94
Halo	10 x 0.21	20	1.00	15700	80

Measurement of band broadening of Acquity Classic UPLC

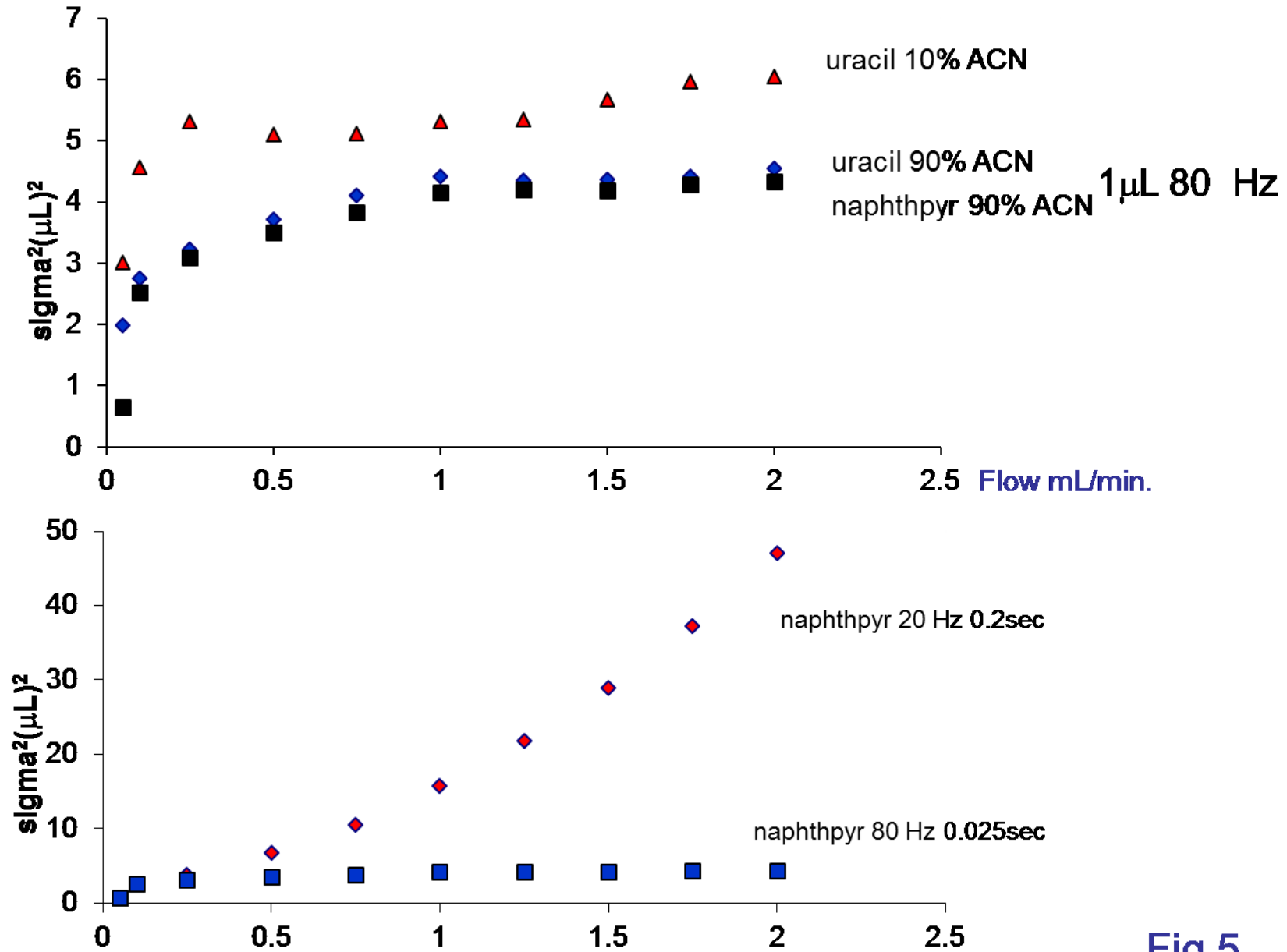
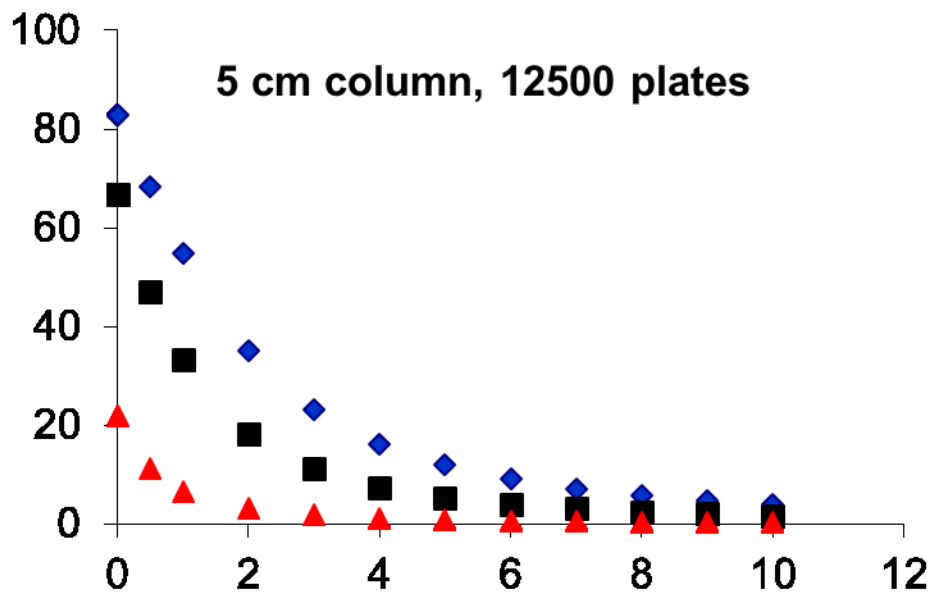
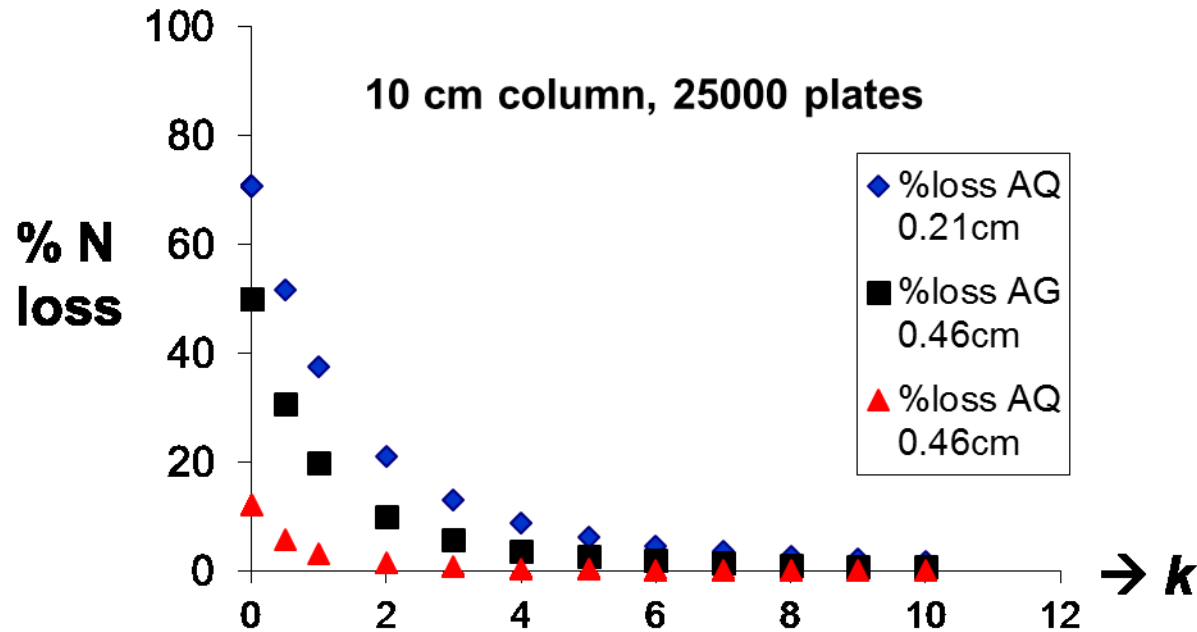


Fig.5

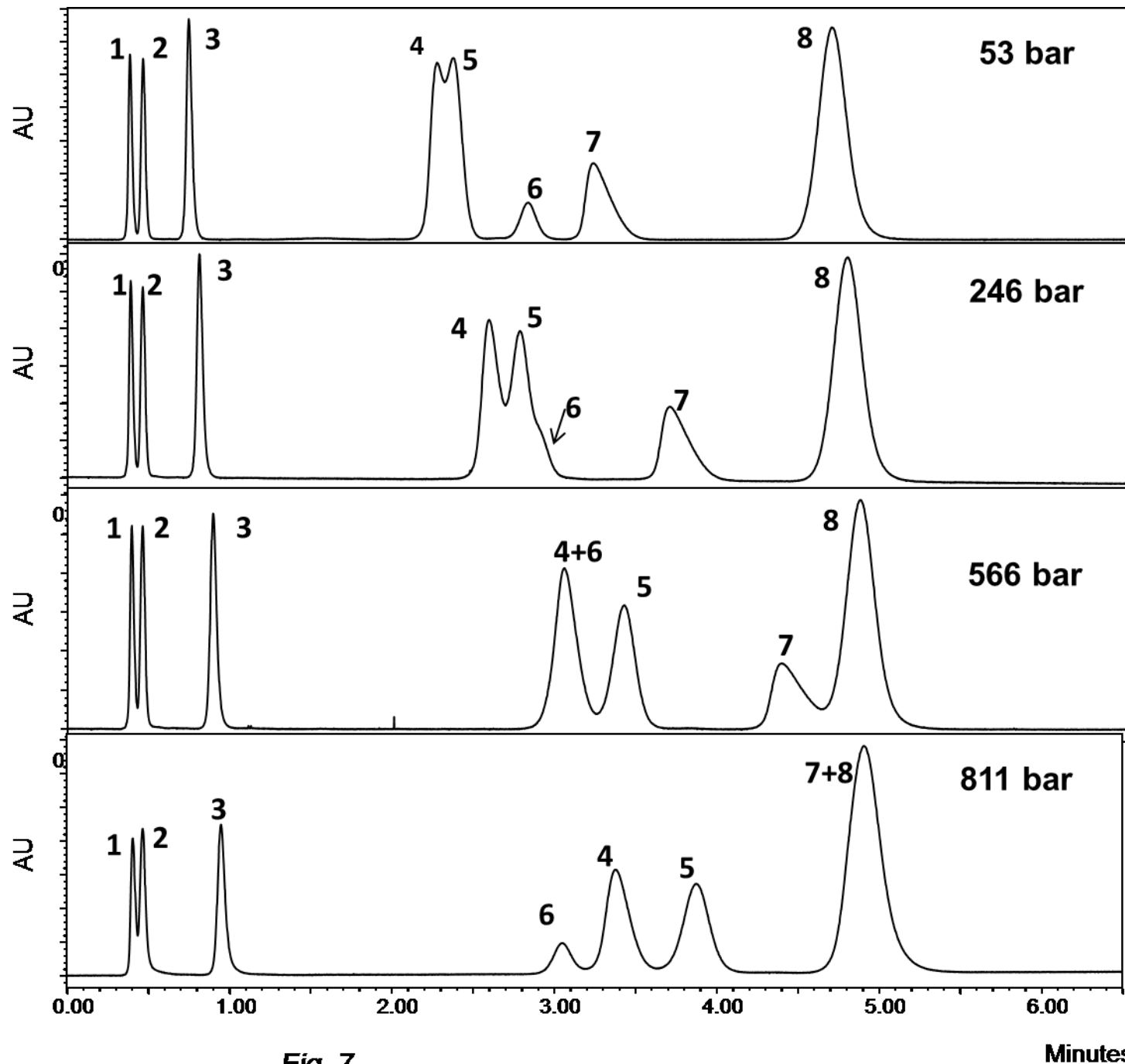
Comparison of Efficiency loss due to instrumental band broadening-using naphthopyrene data 90 %ACN



AQ= Acquity $\sigma^2 = 3.5 \mu\text{L}^2$

AG= Agilent 1100 $\sigma^2 = 25 \mu\text{L}^2$

Fig. 6



Changes in Selectivity with Pressure

- 1= uracil
- 2= aniline
- 3= naphthalene 2 sulfonic acid
- 4 = propranolol
- 5 = prednisone
- 6= acetophenone
- 7= diphenhydram.
- 8 = nitrobenzene

C18 column;
mobile phase 25 %
ACN in phosphate
buffer pH 2.7

Fig. 7

Fig 8

**SEM of a hybrid
organic silica
monolith**

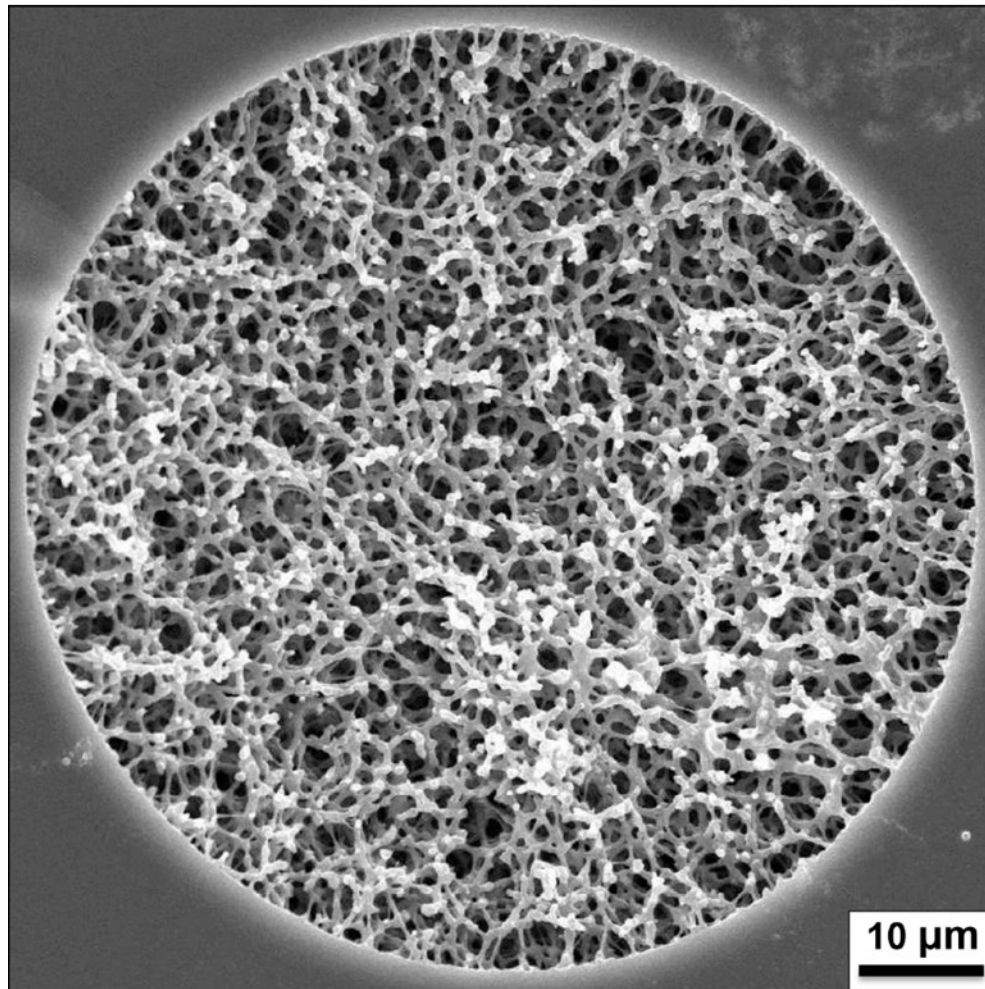
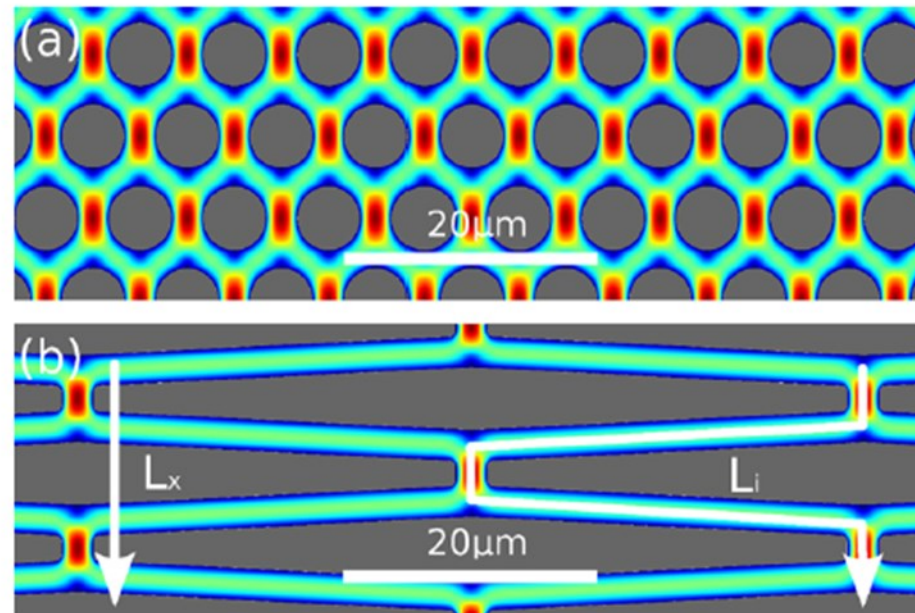


Fig. 9



Top view of pillar arrangement and velocity field of (a) a conventional cylindrical pillar array column and (b) a radially elongated pillar column. The white arrow L_x indicates the net direction of flow; white arrow L_i indicates the direction of flow along the tortuous path followed by the liquid.